Schottky solar cells based on graphene nanoribbon/multiple silicon nanowires junctions

Chao Xie, Jiansheng Jie, Biao Nie, Tianxin Yan, Qiang Li, Peng Lv, Fangze Li, Mingzheng Wang, Chunyan Wu, Li Wang, and Linbao Luo

Citation: Applied Physics Letters **100**, 193103 (2012); doi: 10.1063/1.4711205
View online: http://dx.doi.org/10.1063/1.4711205
View Table of Contents: http://scitation.aip.org/content/aip/journal/apl/100/19?ver=pdfcov
Published by the AIP Publishing

Schottky solar cells based on graphene nanoribbon/multiple silicon nanowires junctions

Chao Xie,[1,2] Jiansheng Jie,[3,a)] Biao Nie,[1] Tianxin Yan,[1] Qiang Li,[1] Peng Lv,[1] Fangze Li,[1] Mingzheng Wang,[1] Chunyan Wu,[1] Li Wang,[1] and Linbao Luo[1,b)]
[1]*School of Electronic Science and Applied Physics, Hefei University of Technology, Hefei Anhui 230009, People's Republic of China*
[2]*School of Materials Science and Engineering, Hefei University of Technology, Hefei Anhui 230009, People's Republic of China*
[3]*Institute of Functional Nano and Soft Materials (FUNSOM) and Jiangsu Key Laboratory for Carbon-Based Functional Materials and Devices, Soochow University, Suzhou Jiangsu 215123, People's Republic of China*

(Received 6 February 2012; accepted 17 April 2012; published online 7 May 2012)

We report the construction of Schottky solar cells based on graphene nanoribbon/multiple silicon nanowires (SiNWs) junctions. Only a few (~10) SiNWs were involved to miniaturize the solar cell for nanoscale power source applications. It was found that doping level of the SiNWs played an important role in determining the device performance. By increasing the doping level, solar cell with open circuit voltage of 0.59 V and energy conversion efficiency of 1.47% were achieved under AM 1.5G illumination. The large effective junction area of the radial Schottky junction was responsible for the high device performance. © *2012 American Institute of Physics*. [http://dx.doi.org/10.1063/1.4711205]

Solar energy harvesting is one of the most promising processes for clean and renewable power. The past several decades had witnessed the dominant role of commercial single- and poly-crystalline silicon solar cells played in the global photovoltaic market. More recently, one-dimensional (1D) Si nanostructures, such as Si nanowires (SiNWs) and nanoribbons (SiNRs), have attracted increasing research interest by the virtue of their unique optical and optoelectronic properties.[1,2] For instance, Kelzenberg *et al*. reported single SiNW rectifying junction solar cell with energy conversion efficiency of ~0.46%.[3] By using a Pt-SiNW-Al structure, Kim *et al*. demonstrated multiple SiNWs (multi-SiNWs)-embedded Schottky solar cells with a large photocurrent.[4] In addition, solar cell devices composed of radial p-n junction, axial and coaxial p-i-n SiNWs with efficiency of ~0.63%, 0.5%, and 3.4%, respectively, have been fabricated as well.[5–7] Despite these progresses, the relatively low efficiencies as well as the complicated fabrication process largely hinder their applications in solar energy conversion.

In order to increase the conversion efficiency, graphene with many exceptional properties such as high transparency, large thermal conductivity, and excellent electronic and mechanical properties has been adopted to optimize the solar cell devices.[8–10] Ye *et al*. reported CdSe nanoribbon (NR)/graphene Schottky solar cells with efficiency of 1.25%.[11] The efficiency can be further enhanced to 1.65% by using Au/graphene Schottky electrodes.[12] What is more, by combining with the Si wafer or SiNW array, graphene film/Si Schottky solar cells were fabricated, which showed efficiencies in the range of 1.65%-4.35%.[13–16] Considering the importance of nanoscale power sources for future nano-optoelectronics, further investigations on the single or multiple SiNWs based graphene/Si Schottky solar cells are much desired. Study on this topic will be conducive to clarify the work mechanism of the graphene/Si solar cells that is vital important to device optimization. Herein, we report the fabrication of solar cells composed of graphene nanoribbon (GrNR) multi-SiNWs Schottky diodes. It was found the device performance strongly depended on the doping level of the n-type SiNWs, and efficiency up to 1.47% was achieved under AM 1.5G illumination. Moreover, the GrNR/multi-SiNWs Schottky diodes could serve as high-performance photoswitches.

Phosphorus (P)-doped n-type SiNWs were synthesized by chemical vapor deposition (CVD) using a vapor-liquid-solid (VLS) growth method.[17] A mixed gas of SiH_4 (10% in H_2, 50 sccm) and H_2 (40 sccm), together with the PH_3 (1% in H_2) dopant, were used as the reaction gas. During growth, cleaned Si substrates covered with 10 nm Au catalyst were heated up to 580 °C and then maintained at the temperature for 40 min. In this work, three samples with varied doping level were synthesized by changing the PH_3 gas flow ratio to 5, 12, 15 sccm, respectively. Monolayer graphene films were prepared at 1000 °C by using a mixed gas of CH_4 (40 sccm) and H_2 (20 sccm) via a CVD method in which 25 μm thick Cu foils were employed as the catalytic substrates.[18] The graphene films were spin-coated with 5 wt. % polymethylmethacrylate (PMMA) in chlorobenzene after growth, and then the underlying Cu foils were removed in Marble's reagent solution ($CuSO_4$:HCl:H_2O = 10 g:50 ml:50 ml).

Figure 1(a) shows typical scanning electron microscopy (SEM, SIRION 200 FEG) images of the SiNWs. It is seen that the SiNWs are smooth and clean with 50–300 nm in diameter and tens of micrometers in length. As for the synthesized graphene film, two major scattering peaks appear in the Raman spectrum (JY, LabRAM HR800) [Figure 1(b)], i.e., 2D-band peak at ~2690 cm^{-1} and G-band peak at ~1590 cm^{-1}. The intensity ratio of I_{2D}: $I_G \approx 3.7$, along with the weak D-band scattering at ~1347 cm^{-1}, confirms the high quality of the monolayer graphene film.[19]

a)Author to whom correspondence should be addressed. Electronic mail: jason.jsjie@gmail.com.
b)Electronic mail: luolb@hfut.edu.cn.

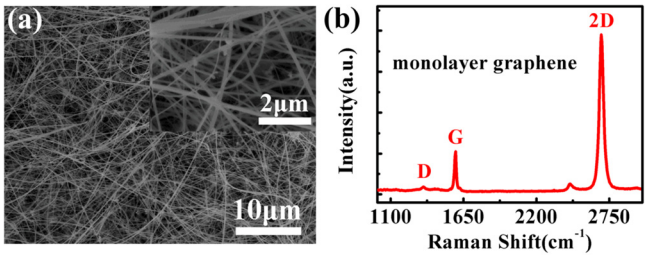

FIG. 1. (a) SEM images of the SiNWs prepared by VLS method. (b) Raman spectrum of the monolayer graphene film.

Figure 2 illustrates the processing steps for constructing GrNR/multi-SiNWs Schottky solar cells. First, Ti/Au (20/40 nm) electrodes were defined by photolithography and subsequent lift-off process on SiO_2 (300 nm)/p^+-Si substrate. The as-synthesized SiNWs were then parallel transferred onto the SiO_2/Si substrate through a contact printing technique during which the NW density could be controlled by adjusting the contact pressure.[20] Second, the Ti (200 nm)/n-SiNWs ohmic contacts were fabricated by additional photolithography and lift-off process. Third, the PMMA-supported monolayer graphene film was transferred onto the SiO_2/Si substrate and dried at 100 °C for 20 min, followed by removing the PMMA with acetone. Finally, the GrNR/multi-SiNWs Schottky solar cells were accomplished by patterning the graphene film with photolithography and oxygen plasma etching for 10 min. Residual photoresist on the GrNRs was then removed by acetone. To improve the p-type conductivity of the GrNRs, the graphene films were pre-treated in HNO_3 solution (65 wt. %) for 5 min and then cleaned in deionized water for several times prior to transfer.[21] It should be noted that, in order to explore the influence of doping level on device performance, totally 3 GrNR/multi-SiNWs Schottky junction solar cells (marked as device A, B, C) were constructed from the SiNWs with different doping levels. Device analysis of the Schottky junction solar cells was conducted on semiconductor characterization system (Keithley 4200-SCS) using the illumination light (350 μW cm^{-2}) as the light source. Further investigations were performed using a solar simulator (San-Ei Electric, XES-301 S) with a calibrated illumination power density of 100 mW cm^{-2}.

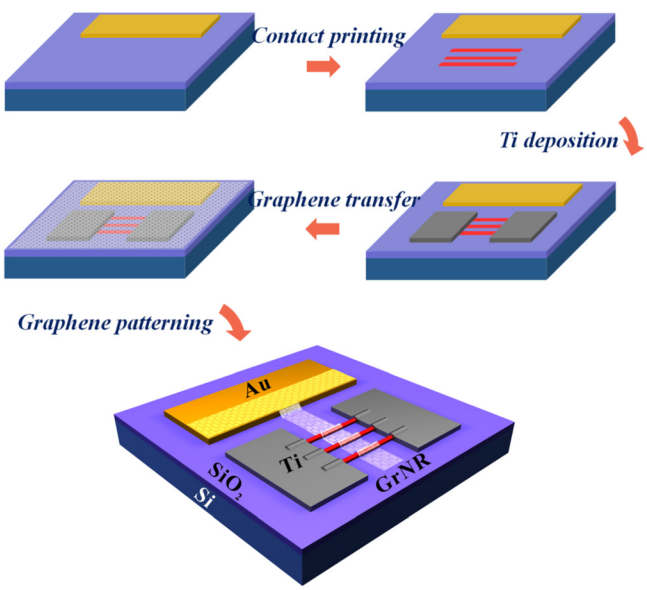

FIG. 2. Schematic illustration of the fabrication process for the GrNR/multi-SiNWs solar cells.

Fig. 3(a) displays a typical SEM image of the GrNR/multi-SiNWs solar cell, in which a few SiNWs, typically 10-15 SiNWs, cross over the GrNR and the Ti electrode. Due to its high flexibility, the GrNR can wrap majority of side surfaces of the SiNWs (Fig. 2), virtually forming a radial Schottky junction structure. Such structural feature will be beneficial to the device performance as the effective junction area for an individual SiNW is much larger than that of the graphene film/SiNW array devices, in which only the tips of the SiNWs can contact with the graphene film.[14] The electrical properties of the SiNWs were first assessed, as depicted in Fig. 3(b). The linear *I-V* curves obtained from the adjacent Ti electrodes indicate the good ohmic contact of n-type SiNWs with Ti electrodes. Also, it is clear that the conductance of the SiNWs is dominated by the P doping and increases with the increasing of doping level. The conductivities of the SiNWs were estimated to be 6.31×10^{-4}, 0.21, 2.1 S/cm for PH_3 flow ratio of 5, 12, 15 sccm, respectively.

Figure 3(c) shows the photovoltaic characteristics of the three devices. Under the white light illumination, all devices exhibit pronounced photovoltaic behavior, but their performances are not identical; device A is the worst, device B the moderate, while device C the best. Interestingly, the open circuit voltage (V_{OC}), along with the short circuit current density (J_{SC}), increases remarkably with the increasing of the SiNW doping level from device A–C. Fill factor (*FF*) and power conversion efficiency (η) of the devices could be deduced from the following equations:

$$FF = I_m V_m / I_{sc} V_{oc} = J_m V_m / J_{sc} V_{oc}, \quad (1)$$

$$\eta = I_m V_m / S P_{in}, \quad (2)$$

where I_m (J_m) and V_m are the current (current density) and voltage at the maximum power output, respectively, S is the active light collection area, which is calculated by summing

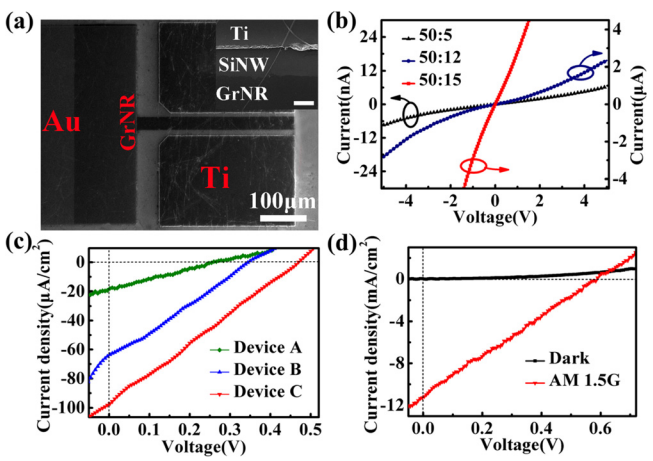

FIG. 3. (a) SEM image of a typical GrNR/multi-SiNWs solar cell. Inset displays single SiNW crossing on GrNR and Ti electrode. The scale bar is 5 μm. (b) Typical *I-V* curves of the SiNWs with varied doping levels. (c) *J-V* curves of GrNR/multi-SiNWs solar cells for devices A, B, C under white light illumination (350 μW cm^{-2}). (d) *J-V* curves of device C measured in dark and under AM 1.5G illumination (100 mW cm^{-2}).

up the diameter of the SiNWs and then multiplying the length covered by the GrNR, and P_{in} is the incident light power density (350 μW cm^{-2}). According to the above equations, *FF* and η are, respectively, estimated to be 0.245 and 0.32% for device A, 0.247 and 1.58% for device B, and 0.261 and 3.44% for device C. It is noted that the device performance of device C at such a light intensity is superior to the best results obtained for monolayer graphene film/SiNW array in our previous work (2.15%).[15] To evaluate the effect of the light power density, the photovoltaic characteristics of device C were examined by a solar simulator (AM 1.5G, 100 mW cm^{-2}). It is found that V_{OC} increases from 0.47 V to 0.59 V, J_{SC} increases from 98.1 μA cm^{-2} to 11.3 mA cm^{-2}, while *FF* slightly decreases from 0.261 to 0.221. Eventually, a η value of 1.47% is obtained. We note J_{SC} is not improved so much although the light source power is increased by near 285 times, which is likely attributed to the large series resistance for the device.

Figure 4(a) shows the photoresponse characteristics of device C at zero bias. It is seen that the device can follow the fast-varying optical signal with a response time less than 20 ms (limited by the instrument) and a response ratio $I_{\text{light}}/I_{\text{dark}}$ of $\sim 10^3$, indicating that the electron-hole pairs could be efficiently generated and separated in the GrNR/multi-SiNWs Schottky solar cells. This result undoubtedly proves the high quality of the junctions. Owing to the excellent stability and reproducibility, the devices may function as high-performance photoswitches. Fig. 4(b) illustrates the energy band diagram of the Schottky solar cell. Because of the work function difference between the p-GrNR and the n-SiNWs, a built-in potential with direction from the SiNW to the GrNR is formed at the junction interface. Under light illumination, photons can easily penetrate the transparent GrNR and irradiate on the SiNWs. Electron-hole pairs will be excited in the SiNWs and then quickly separated by the built-in electric field. The drift of the carriers results in the generation of the photocurrent. For the n-SiNWs with higher doping level, they should have smaller electron work function (Φ_{Si}). In a rough estimation, the work function for device A, B, and C could be deduced to be ~4.47 eV, ~4.29 eV, and ~4.18 eV, respectively.[22] The decrease of the NW work function will lead to a higher Schottky barrier with GrNR and, consequently, the further strengthening of the built-in field; hence, the photogenerated carriers could be separated more efficiently before recombination, giving rise to a superior device performance. The smaller series resistance also contributes to the performance improvement. Above analysis explains why the device performance relied on the doping level of the SiNWs, and is consistent with previous report on the ZnO:Al film/Si heterojunction solar cells.[23] Note that the efficiency of the device under AM 1.5G is still a little bit lower than that of the multi-layer graphene film/SiNW array (~2.86%).[14] The reasons could be ascribed to (1) the large sheet resistance of the monolayer GrNR. (2) inferior light absorption ability for the SiNWs on the plane. Only a small portion of light could be absorbed by the SiNWs, and most of the light is lost through reflection. In contrast, the light absorption in SiNW array is more efficient due to the light trapping effect. However, the larger effective junction area for the GrNR/multi-SiNWs solar cell still guarantees a moderate efficiency for it. It is expected that the device performance could be further improved by enhancing the effective light absorption, reducing the sheet resistance of the GrNR, as well as minimizing the carrier recombination via surface modification.[24]

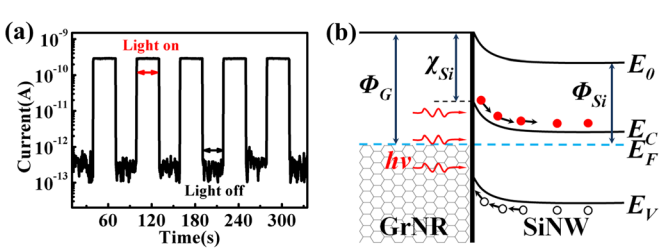

FIG. 4. (a) Photoresponse of device C at zero bias. (b) Energy band diagram of GrNR/SiNW Schottky junction upon light illumination. Φ_G/Φ_{Si} and E_F denote the work functions and Fermi energy level of GrNR/SiNW, respectively. χ_{Si} is the electron affinity of silicon. E_C and E_V are the conduction band and valence band of silicon, respectively.

In conclusion, GrNR/multi-SiNWs Schottky solar cells were fabricated and their photovoltaic characteristics were systemically investigated. By increasing the doping level of the n-type SiNWs, solar cell with a large V_{OC} of 0.59 V and photoconversion efficiency up to 1.47% was achieved. The devices also shows great potential as high-sensitive and fast-responsive photoswitches. Our results demonstrate the promise of GrNR/multi-SiNWs Schottky solar cells in the applications of nano-optoelectronic devices.

This work was supported by the Major Research Plan of the National Natural Science Foundation of China (No. 91027021), National Basic Research Program of China (973 Program, No. 2012CB932400), Program for New Century Excellent Talents in Universities of the Chinese Ministry of Education (No. NCET-08-0764), and National Natural Science Foundation of China (NSFC, Nos. 51172151, 60806028, 21101051, 61106010, and 20901021).

[1]A. J. Baca, M. A. Meitl, H. C. Ko, S. Mack, H.-S. Kim, J. Y. Dong, P. M. Ferreira, and J. A. Rogers, Adv. Funct. Mater. **17**, 3051 (2007).
[2]J. S. Jie, W. J. Zhang, K. Q. Peng, G. D. Yuan, C. S. Lee, and S. T. Lee, Adv. Funct. Mater. **18**, 3251 (2008).
[3]M. D. Kelzenberg, D. B. Turner-Evans, B. M. Kayes, M. A. Filler, M. C. Putnam, N. S. Lewis, and H. A. Atwater, Nano Lett. **8**, 710 (2008).
[4]J. D. Kim, J.-H. Yun, C.-S. Han, Y. J. Cho, J. H. Park, and Y. C. Park, Appl. Phys. Lett. **95**, 143112 (2009).
[5]Y. Ke, X. Wang, X. J. Weng, C. E. Kendrick, Y. A. Yu, S. M. Eichfeld, H. P. Yoon, J. M. Redwing, T. S. Mayer, and Y. M. Habib, Nanotechnology **22**, 445401 (2011).
[6]T. J. Kempa, B. Z. Tian, D. R. Kim, J. S. Hu, X. L. Zheng, and C. M. Lieber, Nano Lett. **8**, 3456 (2008).
[7]B. Z. Tian, X. L. Zheng, T. J. Kempa, Y. Fang, N. F. Yu, G. H. Yu, J. L. Huang, and C. M. Lieber, Nature **449**, 885 (2007).
[8]K. S. Novoselov, A. K. Geim, S. V. Morozov, D. Jiang, Y. Zhang, S. V. Dubonos, I. V. Grigorieva, and A. A. Firsov, Science **306**, 666 (2004).
[9]S. P. Pang, Y. Hernandez, X. L. Feng, and K. Mullen, Adv. Mater. **23**, 2779 (2011).
[10]C. X. Guo, G. H. Guai, and C. M. Li, Adv. Energy Mater. **1**, 448 (2011).
[11]Y. Ye, L. Gan, L. Dai, Y. Dai, X. F. Guo, H. Meng, B. Yu, Z. J. Shi, K. P. Shang, and G. G. Qin, Nanoscale **3**, 1477 (2011).
[12]Y. Ye, Y. Dai, L. Dai, Z. J. Shi, N. Liu, F. Wang, L. Fu, R. M. Peng, X. N. Wen, Z. J. Chen, Z. F. Liu, and G. G. Qin, ACS Appl. Mater. Interfaces **2**, 3406 (2010).
[13]X. M. Li, H. W. Zhu, K. L. Wang, A. Y. Cao, J. Q. Wei, C. Y. Li, Y. Jia, Z. Li, X. Li, and D. H. Wu, Adv. Mater. **22**, 2743 (2010).
[14]G. F. Fan, H. W. Zhu, K. L. Wang, J. Q. Wei, X. M. Li, Q. K. Shu, N. Guo, and D. H. Wu, ACS Appl. Mater. Interfaces **3**, 721 (2011).

[15]C. Xie, P. Lv, B. Nie, J. S. Jie, X. W. Zhang, Z. Wang, P. Jiang, Z. Z. Hu, L. B. Luo, Z. F. Zhu, L. Wang, and C. Y. Wu, Appl. Phys. Lett. **99**, 133113 (2011).
[16]Z. Li, H. W. Zhu, D. Xie, K. L. Wang, A. Y. Cao, J. Q. Wei, X. Li, L. L. Fan, and D. H. Wu, Chem. Commun. **47**, 3520 (2011).
[17]S. Sharma, T. I. Kamins, and R. S. Williams, J. Cryst. Growth **267**, 613 (2004).
[18]X. S. Li, W. W. Cai, J. H. An, S. Y. Kim, J. H. Nah, D. X. Yang, R. Piner, A. Velamakanni, I. W. Jung, E. Tutuc, S. K. Banerjee, L. Colombo, and R. S. Ruoff, Science **324**, 1312 (2009).
[19]A. Reina, X. T. Jia, J. Ho, D. Nezich, H. Son, V. Bulovic, M. S. Dresselhaus, and J. Kong, Nano Lett. **9**, 30 (2009).
[20]Z. Y. Fan, J. C. Ho, T. Takahashi, R. Yerushalmi, K. Takei, A. C. Ford, Y. L. Chueh, and A. Javey, Adv. Mater. **21**, 3730 (2009).
[21]S. K. Bae, H. K. Kim, Y. B. Lee, X. F. Xu, J. S. Park, Y. Zheng, J. Balakrishnan, T. Lei, H. R. Kim, Y. I. Song, Y. J. Kim, K. S. Kim, B. Ozyilmaz, J. H. Ahn, B. H. Hong, and S. Iijima, Nat. Nanotechnol. **5**, 574 (2010).
[22]E. K. Liu, B. S. Zhu, and J. S. Luo, *Semiconductor Physics* (Publishing House of Electronics Industry, Beijing, China, 2003).
[23]W. Y. Zhang, Z. Z. Liu, Y. X. Han, and Z. X. Fu, Optoelectron. Adv. Mater.-Rapid Comm. **4**, 681 (2010).
[24]Y. P. Dan, K. Y. Seo, K. H. Takei, J. H. Meza, A. Javey, and K. B. Crozier, Nano Lett. **11**, 2527 (2011).